KERNFORSCHUNGSZENTRUM

KARLSRUHE

September 1971

KFK 1457

Institut für Angewandte Kernphysik
Projekt Schneller Brüter

A Measurement of the Capture – to – Fission Ratio α for ^{235}U and ^{239}Pu with a New Technique

R. E. Bandl, H. Miessner and F. H. Fröhner

GESELLSCHAFT FUR KERNFORSCHUNG M.B.H.

KARLSRUHE

GESELLSCHAFT FÜR KERNFORSCHUNG M.B.H.
KARLSRUHE

KERNFORSCHUNGSZENTRUM KARLSRUHE

September 1971 KFK 1457

Institut für Angewandte Kernphysik
Projekt Schneller Brüter

A Measurement of the Capture - to - Fission Ratio α for ^{235}U and ^{239}Pu with a New Technique+

by

R.-E. Bandl, H. Miessner and F.H. Fröhner

+Presented at the "Third Conference on Neutron Cross Sections and Technology", March 1971, Knoxville, Tennessee

Gesellschaft für Kernforschung mbH Karlsruhe

ABSTRACT

The shape of α, the ratio of capture to fission cross section, has been measured for ^{235}U and ^{239}Pu in the neutron energy range from 8 to 60 keV. A pulsed neutron beam from a ^{7}Li Van de Graaff source was used. The absorption was found by a comparison of the scattered neutrons from the fissile sample with those from a non-absorbing lead sample. The fast fission neutrons were simultaneously detected with an organic liquid scintillator.

Der Verlauf von α, dem Verhältnis von Einfang - zu Spaltquerschnitt, wurde für ^{235}U und ^{239}Pu als Funktion der Neutronenenergie zwischen 8 und 60 keV gemessen. Ein gepulster Neutronenstrahl von einer ^{7}Li-Van-de-Graaff Quelle wurde verwendet. Der Vergleich zwischen den Neutronen, die von einer spaltbaren Probe und denen, die von einer nicht absorbierenden Blei-Probe gestreut wurden, ergab die Absorption. Die schnellen Spaltneutronen wurden gleichzeitig von einem organischen Flüssigkeitsszintillator registriert.

1. Introduction

In spite of their importance for fast-breeder design the capture-to-fission ratio, α, and the number of fission neutrons emitted per neutron absorbed, η , are still not very accurately known in the low keV region. The quantities α and η are defined as

$$\alpha = \frac{\sigma_\gamma}{\sigma_f}, \quad \eta = \bar{\nu}\,\frac{\sigma_f}{\sigma_a}, \qquad (1a, 1b)$$

where σ_γ, σ_f, σ_a are the neutron cross-sections for capture, fission and absorption, respectively, and $\bar{\nu}$ is the average number of neutrons emitted per fission.
Large discrepancies exist between the data from different laboratories even for the main fissile isotopes, ^{239}Pu and ^{235}U (refs. 1 to 6).

A measurement of the shapes of η and α versus neutron energy for ^{239}Pu and ^{235}U between 8 and 60 keV is reported in the present paper. A new technique based solely on neutron detection was employed. The method is similar to measurements below 200 eV of Farley [7], Palevsky et al. [8] and Brooks et al.[9]. These authors exploited the fact that at low energies scattering is much less probable than absorption, so that nearly all neutrons interacting with the sample are absorbed. Thus η can be obtained by a simultaneous measurement of the incident neutron flux, the transmission and the yield of fission neutrons.

In the keV region, however, scattering exceeds absorption and must be taken into account. This is realized in the present experiment by an additional measurement of the neutron flux escaping from the sample after scattering.

2. Method

For a sample of fissile material the neutron absorption rate R_a and the number of fission neutrons N_f per second are given by

$$R_a = \phi_o \left\langle (1-T^f) \left[\frac{\sigma_a}{\sigma} + \frac{\sigma_s}{\sigma} (1-T') \left[\frac{\sigma_a'}{\sigma'} + \frac{\sigma_s'}{\sigma'} (1-T'') \left[\ldots \right] \right] \right] \right\rangle \qquad (2)$$

$$N_f = \bar{\nu}\, \phi_o \left\langle (1-T^f) \left[\frac{\sigma_f}{\sigma} + \frac{\sigma_s}{\sigma} (1-T') \left[\frac{\sigma_f'}{\sigma'} + \frac{\sigma_s'}{\sigma'} (1-T'') \left[\ldots \right] \right] \right] \right\rangle \qquad (3)$$

where ϕ_o is the incident neutron flux, T^f the transmission of the fissile sample, and σ, σ_s are the total and scattering cross-sections respectively. The triangular brackets denote averages over many resonances, the primed symbols are valid for reactions after the first, second etc. scattering process. The ratios η and α can be written

$$\bar{\nu} \frac{\langle \sigma_f \rangle}{\langle \sigma_a \rangle} = \frac{N_f}{R_a} \cdot k, \quad \frac{\langle \sigma_\gamma \rangle}{\langle \sigma_f \rangle} = \frac{\bar{\nu}\, R_a}{k\, N_f} - 1 \qquad (4a, 4b)$$

where k is a correction factor for multiple scattering and resonance self-shielding. Note, that η and α are independent of multiple scattering, if the cross sections change smoothly with energy.

The absorption rate can be written as

$$R_a = \phi_o \langle 1-T^f \rangle - \langle \phi_s^f \rangle \qquad (5)$$

where ϕ_s^f is the flux of primary neutrons escaping from the fissile sample after scattering. A measurement of ϕ_s^f requires a 4π detector with exactly the same efficiency as that for the ϕ_o measurement.

This can be avoided by comparing the flux of scattered neutrons escaping from an absorbing sample with that escaping from a non-absorbing sample, such as lead, if the transmission of both samples is known.
The counting rates C_s^{Pb} and C_s^f of scattered neutrons from a lead and a fissile sample, as measured by a neutron detector with efficiency ε, are given by

$$C_s^{Pb} = \frac{\varepsilon \Omega}{4\pi} \cdot \phi_o \, (1-T^{Pb}) \qquad (6)$$

$$C_s^f = \frac{\varepsilon \Omega}{4\pi} \langle \phi_s^f \rangle \qquad (7)$$

where Ω is the solid angle between sample and neutron detector. Using Eqs. (6) and (7), Eq. (5) becomes

$$R_a = \frac{4\pi}{\varepsilon \Omega} \left(C_s^{Pb} \frac{\langle 1-T^f \rangle}{1-T^{Pb}} - C_s^f \right). \qquad (8)$$

This equation implies an isotropic angular distribution of the scattered neutrons, which is not valid. A correction must therefore be applied to the scattered neutron yields (see sect. 4).

The counting rate C_f of fission neutrons measured by a fast neutron detector is proportional to N_f, since the angular distribution and the energy spectrum of the fission neutrons can be assumed to be independent of the incident neutron energy in the energy range considered here.

In the present experiment the counting rate C_f of a fast neutron detector and the counting rates C_s^f and C_s^{Pb} of a 1/v detector were measured under identical experimental conditions as a function of incident neutron energy E_n. In a second run the transmissions T^f and T^{Pb} of the fissile and lead sample, respectively, were measured as a function of energy. In terms of these quantities Eq. (4b) can be written as

$$\frac{\langle \sigma_\gamma \rangle}{\langle \sigma_f \rangle} = \text{const.} \; \frac{\sqrt{E_n}\,\left(C_s^{Pb}\,\frac{\langle 1-T^f \rangle}{1-T^{Pb}} - C_s^f\right)}{C_f \cdot k} - 1 \; ; \qquad (9)$$

$\bar{\nu}$ is assumed to be constant in the energy range of the present experiment.

3. Experimental Setup

A broad neutron spectrum with energies from 5 to 70 keV was produced via the $^7Li(p,n)^7Be$ reaction at a 3 MV pulsed Van de Graaff accelerator (pulse length after bunching: 1 ns). The energy of the incident neutrons was determined by the time-of-flight method. Since the neutrons produced in this energy range are collimated kinematically within about $\pm 30^\circ$, neither beam collimation nor detector shielding was necessary. All samples used in the measurement were 4 cm diameter metal discs, 0.035 to 0.05 atoms/barn thick, and packaged identically in 0.2 mm thick copper. The three samples (Pu, U and Pb) together with an empty copper can were mounted on a sample changer 14 cm distant from the neutron-producing target (Fig. 1). The scattered neutrons were registered by a ^6Li-glass scintillator (NE 905) of 1.2 cm thickness and 11 cm diameter coupled to an XP 1040 photomultiplier. The efficiency of this detector for fission neutrons is small. An identical detector with a neutron insensitive ^6Li-depleted glass scintillator (NE 906) served for γ-ray background determination.

A proton recoil detector measured the prompt fission neutrons. It consisted of a liquid scintillator (NE 213) with 3 cm thickness and 11 cm diameter viewed by an XP 1040 photomultiplier with pulse shape discrimination against γ-radiation[10].

The transmission measurements were performed in a separate run with a ^{6}Li-glass detector and a paraffin collimator between the sample and the detector.

The overall time resolution of this experimental arrangement was 20 ns/m and the energy resolution was 10 % at 30 keV neutron energy.

4. Corrections

The scattered neutron yield must be corrected for inelastic scattering in the fissile sample and for the detection of fast fission neutrons by the ^{6}Li-glass detector. These two corrections were calculated from given cross sections [11] and found to be less than 3 % each.
The γ-ray background, as measured by the γ-sensitive detector, was subtracted from the scattered neutron time-of-flight spectrum. This correction amounted to 1 % or less.

The correction due to the energy-dependent angular distribution of the scattered neutrons was calculated by means of a Monte Carlo program. The resulting corrections were between 2 % and 13 % in the scattered neutron flux for the various angles under which scattering has been measured. The deviation from isotropy is mainly caused by the sample geometry and less by p-wave scattering (differential scattering cross sections were obtained from refs. [12,13]).
The neutron absorption of lead [14] and the γ-ray response of the proton recoil detector were found to be negligible.

Since the transmissions of the lead and the fissile samples were nearly equal, the error due to background correction in the scattered neutron spectrum was small. The reason is that only the differences between the scattering counting rates of the two samples enter into Eq. (8). The time-of-flight spectra from the scattering and transmission measurements were broadened numerically so that they corresponded to the same energy resolution as the fission neutron data. The shape of α was corrected for small deviations of the efficiency from a 1/v behaviour of the ^{6}Li glass detector [15,16]. The correction factor k has been found by means of a Monte Carlo code [17] to differ less than 1 % from unity in the energy range of interest. The corrections in α due to impurities of the samples were less than 3 %. The estimated uncertainties are shown in Table 1.

Table 1. Uncertainties in α

		10 keV	20 keV	50 keV
^{239}Pu	systematic	± 12 %	± 10 %	± 11 %
	statistical	± 10 %	± 8 %	± 5 %
	total	± 16 %	± 13 %	± 12 %
^{235}U	systematic	± 13 %	± 10 %	± 10 %
	statistical	± 11 %	± 8 %	± 4 %
	total	± 17 %	± 13 %	± 11 %

5. Results and discussion

The ^{239}Pu α data were normalized to the values of de Saussure et al. [1] in the energy range from 40 to 50 keV, while the ^{235}U α data were normalized in the same energy range to the recommended values of Alter and Dunford [18]. The results, together with those of other laboratories (ref. 1 to 6 and ref. 20) are shown in Figs. 2 and 3. It should be pointed out that the normalization for ^{239}Pu was performed with values given in a table by de Saussure et al. [1] and not with the averaged values shown in Fig. 2. The normalization error, which is estimated to be 10 % for both ^{239}Pu and ^{235}U, is not included in Table 1.

The numerical results of α for ^{239}Pu and ^{235}U are listed in Table 2.

Table 2. Ratio of Capture to Fission for ^{239}Pu and ^{235}U.

Energy Range (keV)	$\frac{\langle \sigma_\gamma \rangle}{\langle \sigma_f \rangle}$ of ^{239}Pu	$\frac{\langle \sigma_\gamma \rangle}{\langle \sigma_f \rangle}$ of ^{235}U
8.0 - 9.0	0.687	0.402
9.0 - 10.0	0.689	0.337
10.0 - 11.0	0.617	0.374
11.0 - 12.0	0.604	0.406
12.0 - 13.0	0.505	0.353
13.0 - 14.0	0.539	0.335
14.0 - 15.0	0.566	0.437
15.0 - 16.0	0.450	0.453
16.0 - 17.0	0.381	0.415
17.0 - 18.0	0.386	0.371
18.0 - 19.0	0.389	0.343
19.0 - 20.0	0.388	0.362
20.0 - 22.5	0.354	0.349
22.5 - 25.0	0.304	0.279
25.0 - 27.5	0.287	0.269
27.5 - 30.0	0.284	0.278
30.0 - 35.0	0.291	0.324
35.0 - 40.0	0.280	0.346
40.0 - 45.0	0.244	0.333
45.0 - 50.0	0.236	0.371
50.0 - 60.0	0.218	0.364

Below 15 keV our ^{239}Pu data are significantly higher than the results of Gwin et al. [4] and tend more toward those of Schomberg et al. [2]. The structure in the shapes of α for both ^{239}Pu and ^{235}U is believed to be significant because it was reproduced in three independent runs. The structure around 14 keV in α for ^{239}Pu is similar to that in the bomb-shot data of Farrell et al. [20]. It may indicate intermediate structure in the fission cross-section due to subthreshold fission [19].

REFERENCES

1. G. de Saussure et al., Nucl. Data for Reactors II, p. 233, IAEA, Vienna (1967)

2. M.G. Schomberg et al., 2nd Intern. Conference on Nucl. Data for Reactors I, 315, IAEA, Helsinki (1970)

3. J.B. Czirr, J.S. Lindsey, 2nd Intern. Conference on Nucl. Data for Reactors I, 331, IAEA, Helsinki (1970)

4. R. Gwin et al., ORNL-TM-2598 (1969)

5. L.W. Weston, G. de Saussure, R. Gwin, Nucl. Science and Engineering, 20, 80 (1964)

6. Van Shi-Di et al., Phys. and Chemistry of Fission I, 287, IAEA, Vienna (1965)

7. F.J.M. Farley, J. Nuclear Energy, 3, 33 (1956)

8. H. Palevsky, D.J. Hughes, R.L. Zimmermann, R.M. Eisberg, J. Nuclear Energy, 3, 177 (1956)

9. F.D. Brooks, J.E. Jolly, M.G. Schomberg, M.G. Sowerby, AERE-M 1670 (1966)

10. R.-E. Bandl, KFK 1458 (1971)

11. I. Langner, J.J. Schmidt, D. Woll, KFK 750 (1968)

12. Yu. A. Aleksandrov, Intern. Nuclear Phys. Conference, 378, Gatlinburg (1966)

13. M.C. Bertin et al. United Nucl. Corpor. 5099 (1964)

14. M.D. Goldberg et al., BNL 325, Supplement No 2, Vol IIc (1966)

15. H.-O. Zetterström, S. Schwarz, L.G. Strömberg, Nucl. Instr. and Methods, 42, 277 (1966)

16. M.G. Sowerby, B.H. Patrick, C.A. Uttley, K.M. Diment, 2nd Intern. Conference on Nucl. Data for Reactors I, 161, IAEA, Helsinki (1970)

17. F.H. Fröhner, Report GA 8380 (1968)

18. H. Alter, C.L. Dunford, AI-AEC-MEMO-12916 (1970)

19. J.J. Schmidt, KFK 966 (1969)

20. J.A. Farrell, G.F. Auchampaugh, M.S. Moore, P.A. Seeger, 2nd Intern. Conference on Nucl. Data for Reactors I, 543, IAEA, Helsinki (1970)

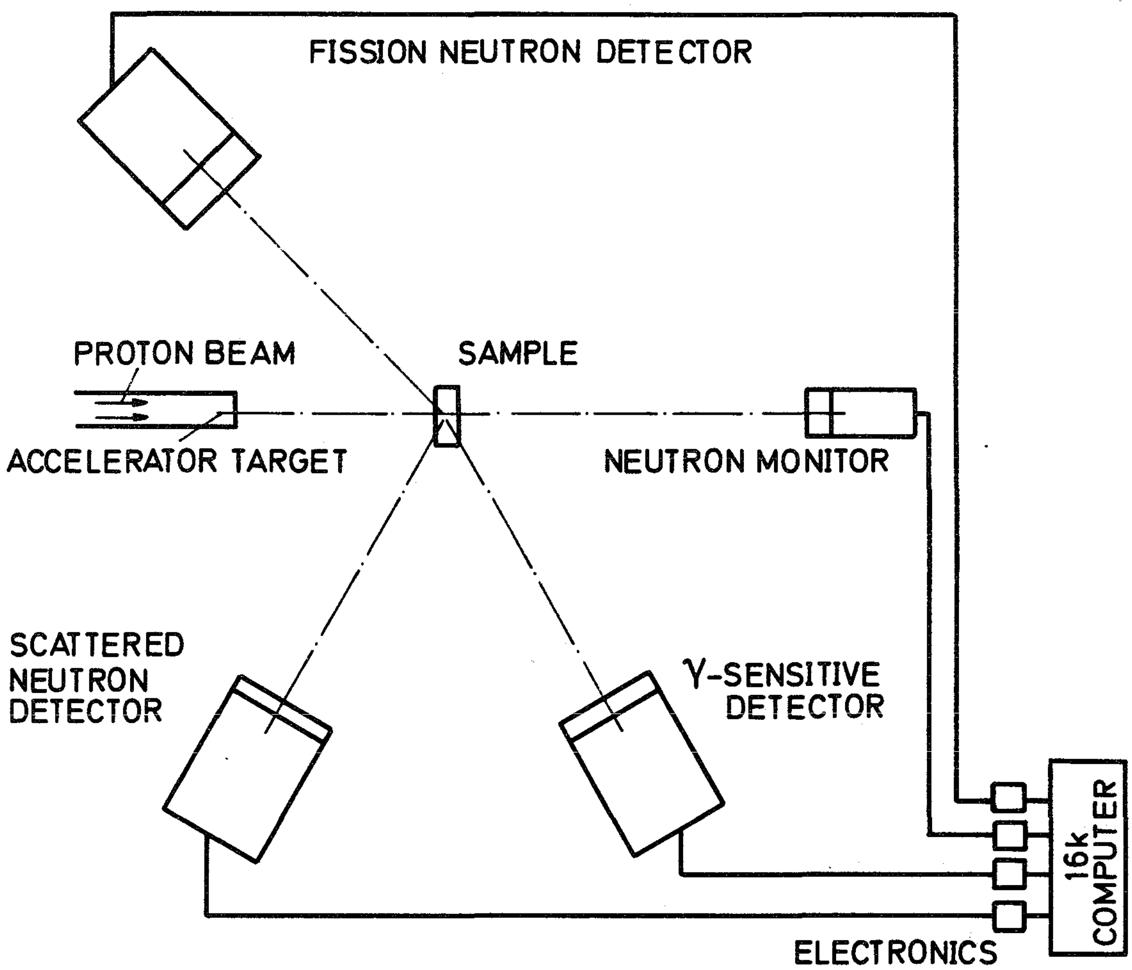

Fig. 1. Experimental Setup (Schematic)

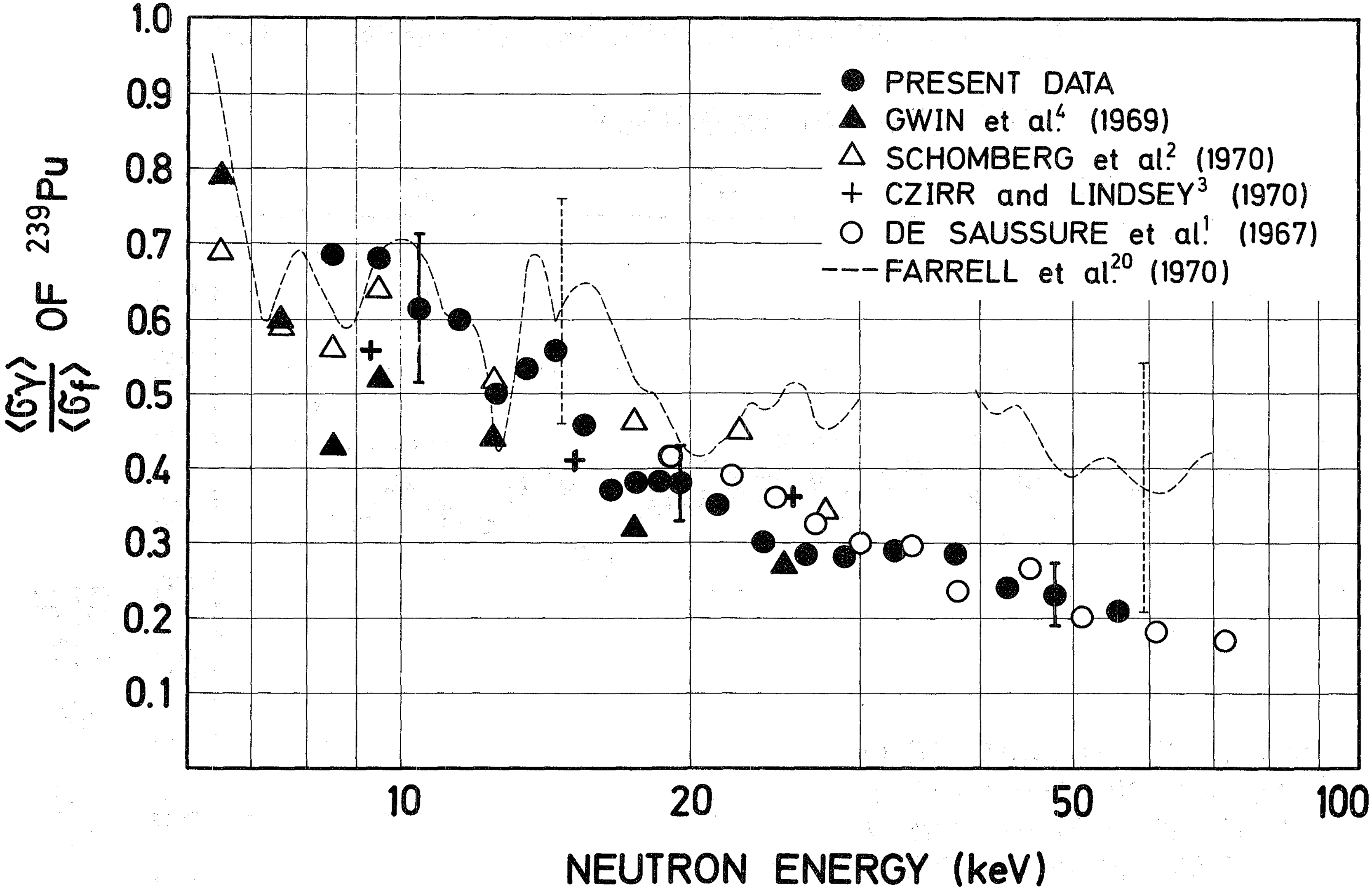

Fig. 2. Ratio of Capture to Fission for ^{239}Pu

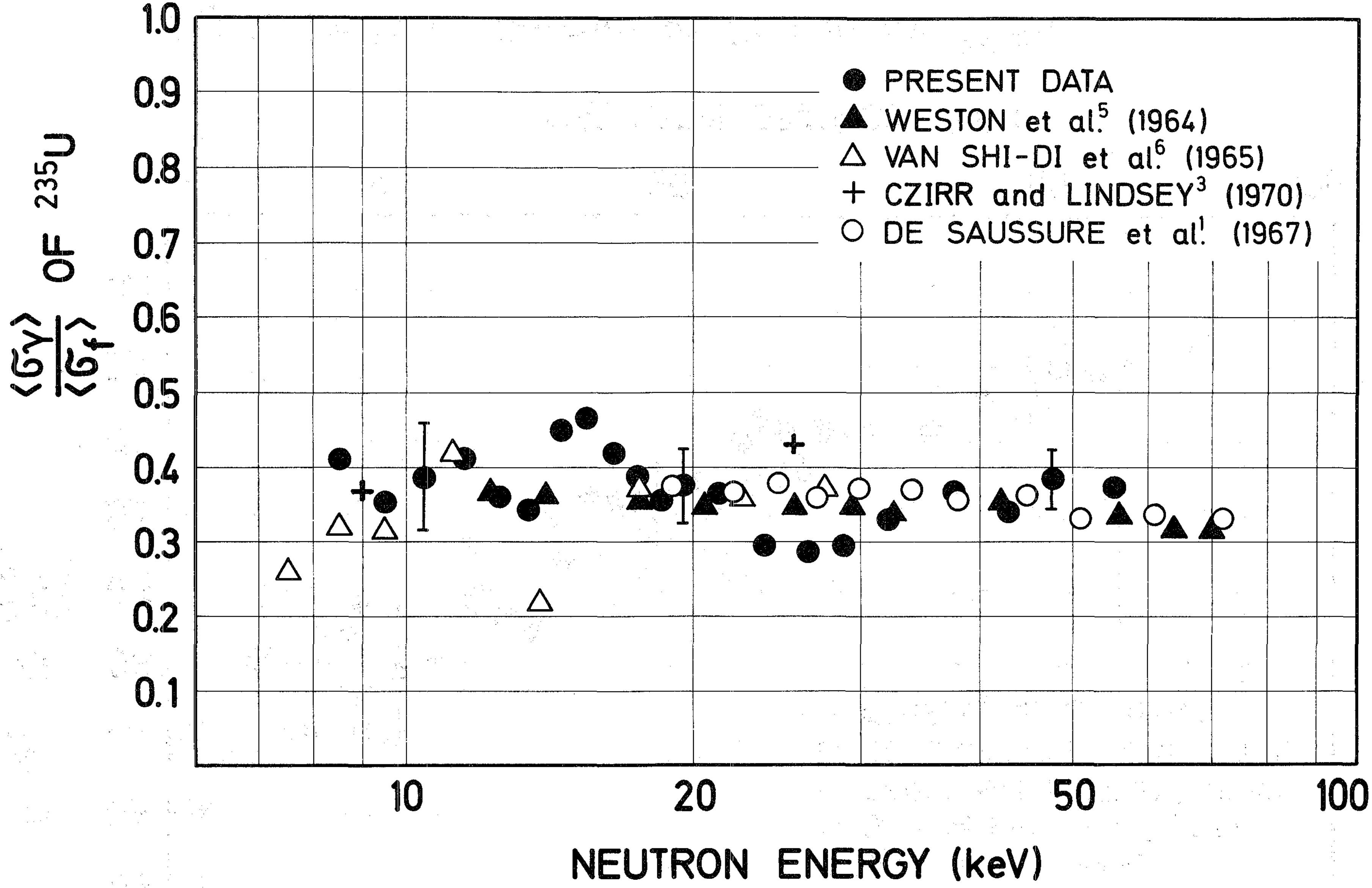

Fig. 3. Ratio of Capture to Fission for ^{235}U